Journal of Hydroscience and Hydraulic Engineering
Vol. 19, No.1 May, 2001, 107-116

TURBULENT STRUCTURES IN OPEN-CHANNEL FLOWS WITH ADVERSE PRESSURE GRADIENTS

By

Iehisa Nezu
Professor, Department of Civil and Global Environment Engineering

Kouki Onitsuka
Research Associate, Department of Civil and Global Environment Engineering
Kyoto University, Kyoto 606-8501, Japan

and

Masaki FUJITA
Kinki Nippon Railway Co., Ltd,.Ue-Honmachi, Tennoji-ku, Osaka, 543-8585, Japan

SYNOPSIS

Turbulence measurements in open-channel flow with adverse pressure gradients were conducted by making use of a laser Doppler anemometer. The friction velocity was evaluated by the linear law in the viscous sublayer. As the results, it was found that the von Karman constant in the log-law is an universal constant in open-channel flow with adverse pressure gradients. In contrast, the integration constant in the log-law and van Driest's damping factor are affected by the adverse pressure gradients. A new relationship formula between the wake strength parameter in the log-wake law and the pressure gradient parameter, based on the friction velocity and the flow depth, is proposed in this study.

INTRODUCTION

Nezu & Rodi(1986) thoroughly investigated on uniform open-channel flows. However, the channel width in natural rivers increases and decreases in the main-flow direction. Investigations on boundary layers with adverse pressure gradient were carried out by several researchers. Clauser(1954) could set-up the equilibrium boundary layers, i.e., the velocity profile is self-similar at all streamwise positions, and indicated that the velocity profiles are controlled by the pressure gradient parameter which is based on the pressure gradient, the friction velocity and the displacement thickness. Mellor & Gibson(1966) measured the equilibrium boundary layers and indicated that the velocity profiles are described by the log-wake law. Coles & Hirst(1968) pointed out that the wake strength parameter depends on the pressure gradient parameter. The empirical formula which described the relationship between the wake strength parameter and the pressure gradient parameter was proposed by White(1974). Recently, Nagano *et al.*(1993) measured adverse pressure gradient boundary layers in the non-equilibrium condition of and made clear that the integration constant in the log-law is affected by the pressure gradient. Further, Spalart & Leonard(1987) showed that the von Karman constant is also affected by the pressure gradient.

Several researches on the adverse pressure gradient open-channel flows were also conducted by a few researchers. Okabe & Sugio(1981) indicated that the mean velocity profiles are described by the log-wake law by making use of a pitot tube. Song & Graf(1994) measured the equilibrium open-channel flows with an acoustic Doppler velocimetry and indicated that the wake-strength parameter depends on the pressure gradient parameter based on the friction velocity and the flow depth. Nezu *et al.*(1994) also presented the relationship between the wake strength parameter and the pressure gradient parameter over a wide range in non-equilibrium open-channel flows. Recently, investigations were carried out not only on mean flow structures, but also on turbulence structures. Song & Graf(1994) and Nezu *et al.*(1994) found experimentally that the Reynolds stress distributions in adverse pressure-gradient open-channel flows take a maximum value at near-half depth. The reason why the Reynolds stress distributions take

Table 1 Hydraulic Condition

case	L(cm)	Q(l/s)	$\sin\theta'$	$\sin\theta$	x=-10(cm)			x=L(cm)		
					h_0(cm)	Fr_0	$Re_0\times10^3$	h_1(cm)	Fr_1	$Re_1\times10^3$
D135-1	135	1.6	1/8000	1/45	4.304	0.14	4.1	7.11	0.067	4.1
D135-2		3.2	1/6000		4.212	0.30	8.1	7.07	0.14	8.1
D135-3		4.8	1/4000		4.151	0.45	12	7.12	0.20	12
D180-1	180	1.6	1/8000	1/60	4.317	0.14	4.5	7.08	0.068	4.5
D180-2		3.2	1/6000		4.292	0.29	8.9	7.08	0.14	8.9
D180-3		4.8	1/4000		4.02	0.48	14	6.938	0.21	14

the maximum there was explained by Song & Graf(1994) by the use of a power law velocity profile under the assumption that the constant in the power law is not affected by the pressure gradient. However, the constant in the power law depends on the flow conditions. Onitsuka *et al.*(1997) verified theoretically that the pressure gradient parameter based on the friction velocity and the flow depth is a dominant parameter and that the Reynolds stress takes the maximum at the near-half depth. In such studies, however, the friction velocity was evaluated by making use of the log-law without any detailed verification. In contrast, Nagano *et al.*(1993) have measured the adverse pressure gradient boundary layer including the viscous sublayer and calculated the friction velocity by both the linear law in the viscous sublayer and the log-law in the inner layer. They pointed out that the evaluation of the friction velocity by the use of the viscous sublayer formula is the most reliable one.

In this study, flow fields in open-channel flows with adverse pressure gradient were measured by making use of a high accuracy two-component fiber-optic LDA.

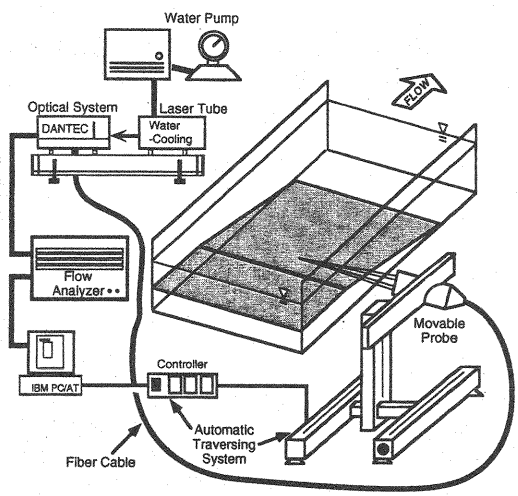

Figure 1 Experimental Setup

EXPERIMENTAL SETUP

The experiments were conducted in a 10-m-long, 40-cm-wide, and 50-cm-deep tilting flume. The decelerated flows were generated by the flat plates as shown in Figure 1. In which x is the streamwise coordinate and y is the coordinate perpendicular to the x direction. L is a length of the deceleration region. The region $x<0$ is called here the "uniform region" and the region of $x>L$ is called the "downstream region". $\sin\theta$ is the channel slope in the deceleration region, and $\sin\theta'$ is that in the uniform and downstream regions. Two components of instantaneous velocities, i.e., the streamwise velocity $\tilde{u}(t)$ and the vertical velocity $\tilde{v}(t)$, were measured with a four-beam LDA system. The present LDA system can measure instantaneous velocities very near the bed, i.e., y =0.1mm. The LDA probe was moved by a computer controlled traversing system. The accuracy of this traversing system was within 1/100mm. All data of the LDA were recorded in a HDD in a personal computer with a sampling frequency with more

than 100(Hz) and sampling time of 60-180s. Variations of water depth in the downstream direction were measured by a digital type point gauge.

The experimental conditions are summarized in Table 1. In which, $Fr \equiv U_m / \sqrt{gh}$ is the Froude number, $Re \equiv U_m h / \nu$ is the Reynolds number, U_m is the bulk mean velocity, g is the gravitational acceleration, h is the flow depth and ν is the kinematic viscosity. The suffice of "0" denotes the value at $x = 0$ and the suffice of "1" denotes the value at $x = L$.

EXPERIMENTAL RESULTS AND DISCUSSION

Evaluation of Friction Velocity

In general, there are several methods to evaluate the friction velocity U_* in non-uniform open channel flows as follows:

i) from the energy gradient I_e

$$U_* = \sqrt{ghI_e} \tag{1}$$

$$I_e = -\frac{d}{dx}\left(\frac{\alpha U_m^{\,2}}{2g} + H\right) \tag{2}$$

in which α is the energy correlation coefficient.

ii) from the momentum equation

iii) direct measurements such as a shear plate

iv) from the linear law in the viscous sublayer($0 \le y^+ \le 5$)

$$U^+ = y^+ \tag{3}$$

in which $U^+ \equiv U / U_*$, $y^+ \equiv y U_* / \nu$.

v) from the log-law in the inner region($30 \le y^+ \le 0.2 R_*$)

$$U^+ = \frac{1}{\kappa} \ln y^+ + A_s \tag{4}$$

in which $R_* \equiv h U_* / \nu$ is the Reynolds number based on the friction velocity, κ is the von Karman constant and A_s is the integration constant.

The accuracy of the methods i) and ii) is not so high, because it is quite difficult to measure the water surface slope dh/dx with high accuracy. Method iii) can measure the friction velocity, but the measured area is not so small, thus the accuracy is not so high. In contrast, method iv) can evaluate the friction velocity theoretically. Nagano *et al.*(1993) have measured the viscous sublayer in the adverse pressure gradient boundary layers and indicated that the method iv) is the most reliable one in the case of adverse pressure gradient boundary layers. In spite of the high accuracy, method iv) has not been used in the adverse pressure gradient open-channel flows except for Nezu *et al.*(1996) and Onitsuka *et al.*(1999), because the turbulence measurements in such thin layers are almost impossible with Pitot tubes and hot-film anemometers. The authors have successfully measured the viscous sublayer by making use of an innovative high-accurate fiber-optic LDA and traversing system.

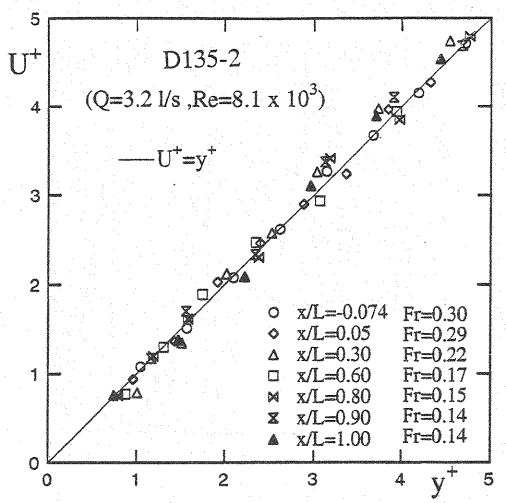

Figure 2 Velocity Profiles in Viscous Sublayer

Figure 2 shows the mean velocity profiles in the viscous sublayer normalized by the friction velocities which were evaluated by Eq.(3). It can be seen that the velocity distributions in the viscous sublayer are in very good agreement with Eq.(3) not only in the uniform region ($x/L < 0$) but also in the deceleration region ($0 \le x/L \le 1.0$). Therefore, the evaluation of friction velocities from Eq.(3) is very reliable in the case of adverse pressure gradient open-channel flows.

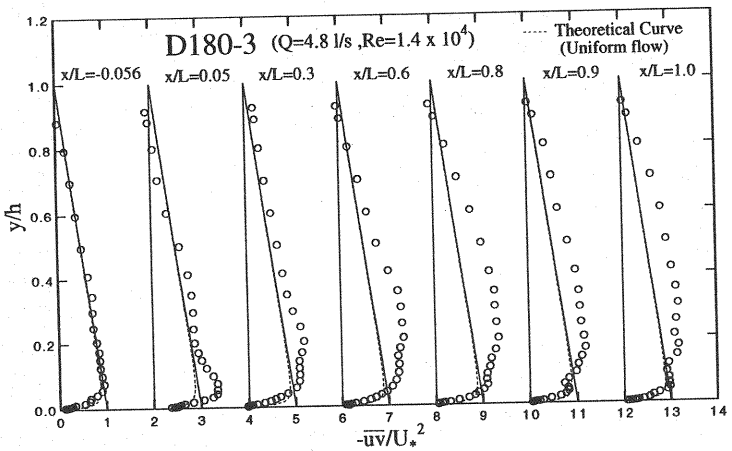

Figure 3 Reynolds Stress Distributions

Reynolds Stress

Figure 3 shows the distributions of the Reynolds stress $-\overline{uv}$ normalized by the friction velocity which is calculated by the linear law in the viscous sublayer(3). In the uniform region, the Reynolds stress distribution corresponds to the theoretical formula in an uniform open-channel flow which is expressed as follows:

$$\frac{-\overline{uv}}{U_*^2} = 1 - \xi - \frac{dU^+}{dy^+} \qquad (5)$$

in which $\xi \equiv y/h$. Therefore, it can be concluded that the flow in the uniform region (x/L =-0.056) is fully developed and that the evaluation of the friction velocity by using Eq.(3) is quite accurate.

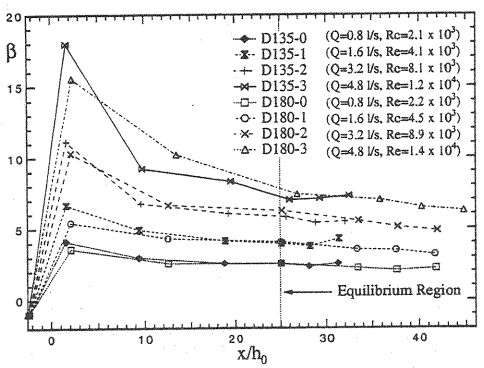

Figure 4 Pressure Gradient Parameter

It can be seen that the flow is re-constructed from the channel bed in the region of $0 \le x/L \le 0.6$. Finally, the distribution of the Reynolds stress are similar at all distances in the region of $0.8 \le x/L \le 1.0$. In such region, the Reynolds stress takes a maximum at near half depth. This results agree with those in adverse pressure gradient (see Mellor & Gibson(1966), Bradshaw(1967) and so on). The reason why the Reynolds stress takes the maximum was verified by Onitsuka *et al.*(1997) semi-theoretically.

Pressure Gradient Parameter

Clauser(1954) used the pressure gradient parameter β_B in analyzing adverse pressure gradient boundary layers as follows:

$$\beta_B = \frac{\delta_*}{\rho U_*^2}\frac{dp}{dx} \qquad (6)$$

in which δ_* is the displacement thickness. In the case of adverse pressure gradient open-channel flows, the flow depth h is used instead of the displacement thickness δ_*. Song & Graf(1994) and Onitsuka *et al.*(1997) used the pressure gradient parameter β as follows:

$$\beta = \frac{h}{\rho U_*^2}\left(-\rho g \sin\theta + \frac{dp}{dx}\right) \qquad (7)$$

$$\frac{dp}{dx} = \rho g \frac{dh}{dx}\cos\theta \qquad (8)$$

Eqs.(6) and (7) mean the characteristics in adverse pressure gradient flows are controlled by the outer variables such as the displacement thickness and the water depth. Figure 4 shows the variations of the pressure parameter β against the flow direction. The value of the pressure gradient parameter β is –1 at the entrance of the decelerated region (x/h_0=0). This implies that the flows in the region of x/h_0<0 are the uniform flow. This is because the β=–1 is obtained theoretically in the case of an uniform open-channel flow by using of $U_* = \sqrt{gh\sin\theta}$. The value of β increases suddenly at the entrance of the decelerated region (x/h_0 =0) and decreases gradually toward downstream. Finally, the value of β becomes almost constant before the exit of the deceleration region (x/h_0>25). Clauser(1954) pointed out that the flow under the condition that the pressure gradient parameter is almost constant is affected only by the pressure gradient. Therefore, such a flow is called the "equilibrium flow". It will be confirmed later that the region of x/h_0>25 is in equilibrium from the velocity profiles in Figure 4.

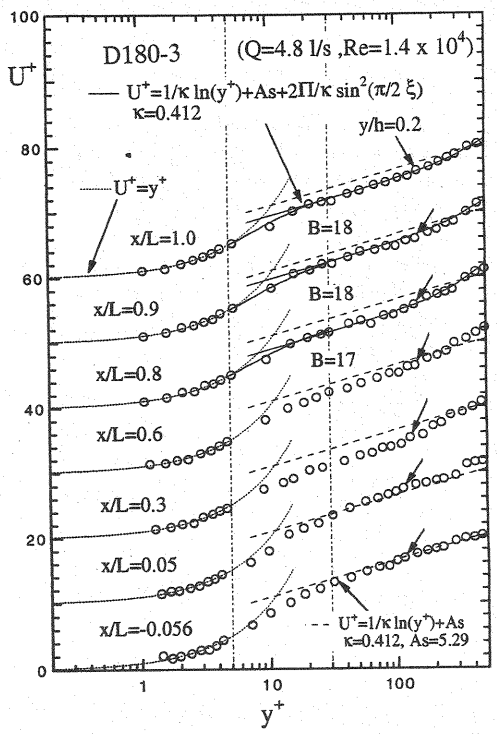

Figure 5 Distributions of Streamwise Velocity

Mean Velocity Distributions

Figure 5 shows mean velocity distributions, together with the log-law(4) as straight lines and the linear law(3) very close to the wall as curved lines in this semi-log plot. In the uniform region (x/L <0), the mean velocity distribution in the inner layer are described well by the log-law(4). In the region of x/L =0.05, however, the values of U^+ deviate upward from the log-law curve. In the region of $0.3 \le x/L \le 0.6$, the variations of U^+ vs. y^+ change in a complicated manner as a function of x, while in the region $0.8 \le x/L \le 1.0$, those are similar in shape. It can be thought that the flows in the region $x/L \le 0.60$ are affected not only by the pressure gradient but also by the upstream flow history. In contrast, the flows in the region $0.8 \le x/L \le 1.0$ is controlled only by the pressure gradient. This region corresponds to the region in which the pressure gradient parameter is almost constant (x/h_0>25, see Figure 4). Therefore, it can be said that the region x/h_0>25 is an "equilibrium region".

It is well known that the mean velocity distributions in the buffer layer ($5 \le y^+ \le 30$) in uniform open-channel flows can be described by the following equation:

$$\frac{dU^+}{dy^+} = \frac{2(1-\xi)}{1+\sqrt{1+4\ell^{+2}(1-\xi)}} \qquad (9)$$

$$\ell^+ = \kappa y^+ \Gamma \qquad (10)$$

$$\Gamma = 1-\exp\left(-y^+/B\right) \qquad (11)$$

in which Γ is van Driest's damping function, B is the damping factor. Eq.(9) is adopted to present flows. It can be seen that the velocity profiles in the viscous sublayer are described by the linear law(3) and those in the buffer layer are described well by the Eq.(9) in the equilibrium region. In the outer region (ξ >0.2), the mean velocity distributions deviate upward from the log-law. Therefore, these are described well by the log-wake law as follows:

$$U^+ = \frac{1}{\kappa}\ln y^+ + A_s + \frac{2\Pi}{\kappa}\sin^2\left(\frac{\pi}{2}\xi\right) \qquad (12)$$

in which Π is the wake strength parameter.

Effects of Pressure Gradient on Various Factors

Nagano *et al.*(1993) investigated on the von Karman constant in adverse pressure gradient boundary layers and indicated that the von Karman constant is not affected by the pressure gradient. In contrast, Spalart & Leonard(1987) pointed out that the von Karman constant is also affected by the pressure gradient in adverse pressure gradient boundary layers. However, the von Kaman constant in adverse pressure gradient open-channel flows has not been investigated at all. It is needed to obtain the value of the friction velocity by a method other than the log-law for evaluating the von Karman constant. In this study, the friction velocity could be evaluated by the linear law(3). Therefore, the von Karman constant in adverse pressure gradient open-channel flows could be investigated for the first time in the present study. Figure 6 shows the variations of the von Karman constant κ against the pressure gradient parameter β in the equilibrium region. Figure 6 also shows Nagano's data in non-equilibrium adverse pressure gradient boundary layers. The Karman constant does not change significantly. In contrast, Nezu & Rodi(1986) made clear that the von Karman constant in uniform open-channel flows (zero pressure gradient flows) is not affected by the Reynolds and Froude number. Therefore, the Karman constant in open-channel flows is independent not only of the Reynolds and Froude number but also of the adverse pressure gradients.

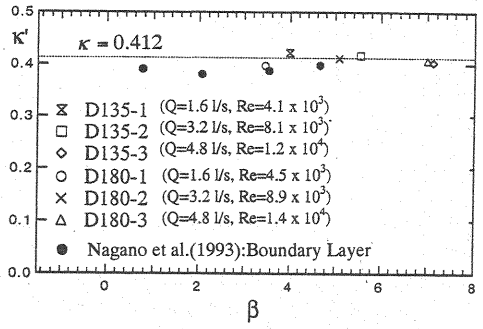

Figure 6 von Karman Constant

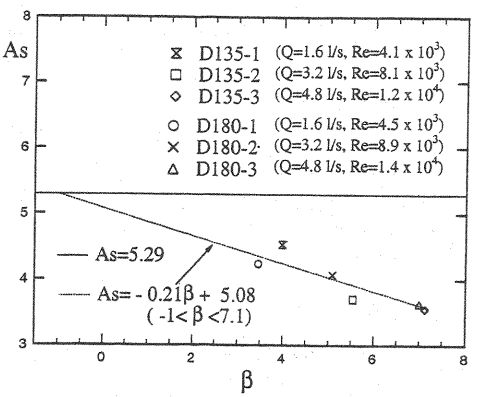

Figure 7 Integration Constant

Nezu & Rodi(1986) showed that the integration constant in the uniform open-channel flows is universal constant irrespective of the Reynolds and Froude number. In contrast, it was pointed out that the integration constant in adverse pressure-gradient open-channel flows is affected by the pressure gradient by Nezu *et al.*(1994). Figure 7 shows the variations of the integration constant A_s in the log-law against β in the equilibrium region. The integration constant decreases with an increase of β. This tendency agrees with that of Nagano's data. An empirical relation between A_s and β is proposed as follows:

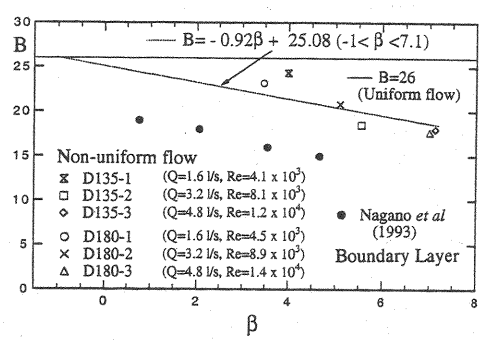

Figure 8 van Driest's Damping Factor

$$A_s = -0.21\beta + 5.08 \quad (-1 \le \beta \le 7.1) \qquad (13)$$

The value of A_s is 5.29 at β =-1(uniform flow), which coincides with Nezu & Rodi's data.

In the case of uniform open-channel flows, the damping factor B is constant(=26). Figure 8 shows the relationship between the damping factor and β in the equilibrium region, together with Nagano's data. Although

both of the present and Nagano's data decrease against β, these do not coincide with each other. This is because the flow of Nagano' experiment is non-equilibrium. Therefore, flow characteristics may be affected by not only by pressure gradient but also by the flow history. The line in Figure 8 is a new experimental formula as follows:

$$B = -0.92\beta + 25.08 \quad (-1 \le \beta \le 7.1) \quad (14)$$

Eq.(14) also shows the value of uniform flows, i.e., B =26 at β =-1.

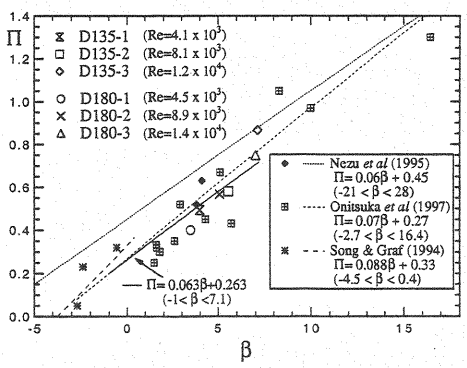

Figure 9 Relationship between Π and β

In the case of zero pressure gradient boundary layers, the velocity profiles in the inner region are described well by the log-law(4). However, those in the outer region deviate from the log-law. Coles(1956) found that those in the outer region are described well by the log-wake law(12) in zero pressure gradient boundary layers. Mellor & Gibson(1966) measured the equilibrium boundary layers and indicated that the velocity profiles are also described by the log-wake law. Coles & Hirst(1968) pointed out that the wake strength parameter depends on the pressure gradient parameter. The empirical formula which described the relationship between the wake strength parameter and the pressure gradient parameter was proposed by White(1974) as follows:

$$\Pi = 0.8(\beta_B + 0.5)^{0.75} \quad (15)$$

Song & Graf(1994) pointed out that the log-wake law is also valid in the outer region in adverse pressure gradient open-channel flows and the wake strength parameter Π depends on the pressure gradient parameter β in equilibrium regions:

$$\Pi = 0.088\beta + 0.33 \quad (-4.5 \le \beta \le 0.4) \quad (16)$$

In their experiments, however, all aspect ratios (=channel width / flow depth) are less than 5 (Nezu & Nakagawa(1993)'s criterion). Therefore, the flow characteristics in their study may be affected not only by the pressure gradient but also by the secondary currents.

Nezu *et al.*(1994) also presented the relationship between Π and β in adverse pressure gradient open-channel flows.

$$\Pi = 0.06\beta + 0.45 \quad (-21 \le \beta \le 28) \quad (17)$$

However, their flow was not in equilibrium.

Onitsuka *et al.*(1997) measured equilibrium open-channel flows by making use of X-type hot-film anemometer and shown the relationship between Π and β.

$$\Pi = 0.07\beta + 0.27 \quad (-2.7 \le \beta \le 16.4) \quad (18)$$

They could not measure the viscous sublayer. As a result, the friction velocity is evaluated by the log-law. However the von Karman constant and integration constant were adopted by the values in uniform open-channel flows (κ =0.412, A_s =5.29). In contrast, Nagano *et al.*(1993) and Nezu *et al.*(1994) pointed out that the integration constant is affected by the pressure gradient. Therefore, the Eq.(18) is not valid. It can be said that there is no empirical formula which describes the relationship between the pressure gradient parameter and the wake strength parameter in equilibrium open-channel flows.

Figure 9 shows the variations of the wake strength parameter Π against the pressure gradient parameter β, together with the data and empirical formulae (16)-(18). It can be seen that the wake strength parameter Π increases with an increase of the pressure gradient parameter β. A new empirical formula is presented here that the flow is in equilibrium as follows:

$$\Pi = 0.063\beta + 0.263 \quad (-1 \le \beta \le 7.1) \quad (19)$$

In the Eq.(19), Π takes 0.2 when β is –1. This coincides with the value in uniform open-channel flows measured by Nezu & Rodi(1986).

Turbulence Intensity

In the case of wall turbulent flows such as boundary layer, pope flow and open-channel flow, it is well known that the turbulence intensity u'/U_* in the viscous sublayer is described by the following equation:

$$\frac{u'}{U_*} = C \cdot y^+ \qquad (20)$$

Nezu & Rodi(1986) and Onitsuka & Nezu(1998) investigated experimentally that the coefficient C is almost constant irrespective of the Reynolds and Froude number in uniform open-channel flows. Figure 10 shows the distributions of turbulence intensity u' normalized by the friction velocity U_* in the viscous sublayer, including Eq.(20) shown by a straight line. In the uniform region (x/L <0), the distributions of the turbulence intensity in the viscous sublayer is described well by Eq.(20). The values of u'/U_* are larger than those of uniform open-channel flows. However, the shape of the distributions is almost linear. The coefficient C is calculated from the Eq.(20) by making use of the least square method. Figure 11 shows the behavior of the coefficients C against β considering C =0.3 at β =-1 in uniform flow, we can obtain the following empirical formula, which is shown in Figure 11.

$$C = 0.011\beta + 0.311 \qquad (-1 \le \beta \le 7.1) \quad (21)$$

Eq.(21) shows that the magnitude of the increase of the turbulence intensity in adverse pressure gradient open-channel flows.

Marusic *et al.*(1997) pointed out that the profiles of turbulence intensity in the buffer and inner layers normalized by inner variables depend on the Reynolds number in zero-pressure gradient boundary layers. In the present flows, the Reynolds number is constant toward downstream. Therefore, the Reynolds number effects can be ignored. Figure 12 shows an example of distributions of u'/U_* near the wall. The curved lines are the semi-theoretical formula which was proposed by Nakagawa & Nezu(1978) as follows:

$$\frac{u'}{U_*} = D_u \exp\left(-\lambda_u \frac{y^+}{R_*}\right)\Gamma + Cy^+(1-\Gamma) \qquad (22)$$

$$\Gamma = 1 - \exp\left(-\frac{y^+}{B_{ut}}\right) \qquad (23)$$

D_u =2.26, λ_u =0.88 and B_{ut} =10 were obtained by Nezu & Rodi(1986). The feature of Eq.(22) is to take the maximum value at y^+ =17. In the uniform region (x/L <0), the turbulence intensity is

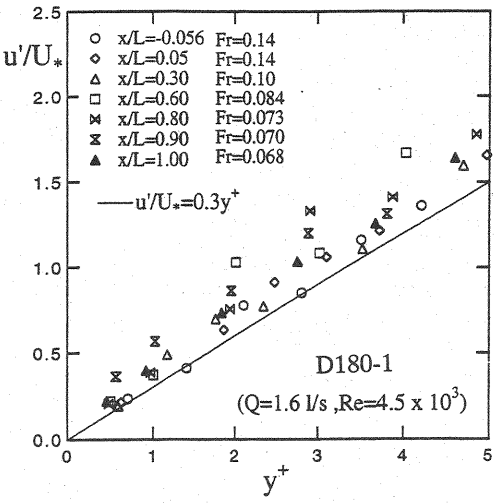

Figure 10 Turbulence Intensity in Viscous Sublayer

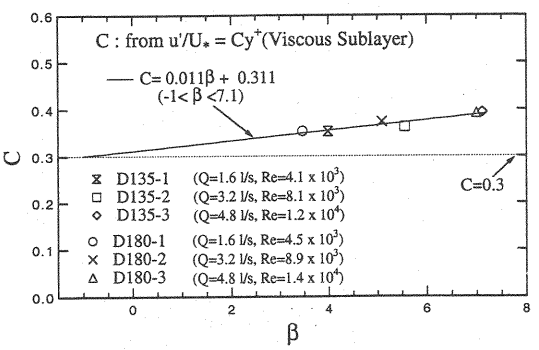

Figure 11 Variations of Coefficient C

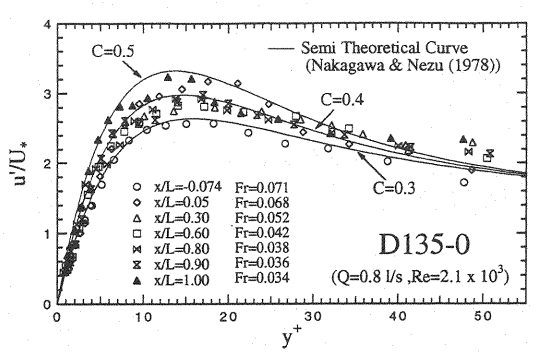

Figure 12 Distributions of Turbulence Intensity near the Bed

described well by the Nakagawa & Nezu's formula. In contrast, the values of u'/U_* increase toward downstream in the decelerated region. The formula of Eq.(22) can described well the experimental data.

Figure 13 shows the distribution of the streamwise turbulence intensity u'/U_* in a whole depth, together with the Nezu & Nakagawa's empirical formula:

$$\frac{u'}{U_*} = D_u \exp(-\lambda_u \xi) \qquad (24)$$

The turbulence intensity takes the maximum very clear to the channel bed in every section. This feature is one of the characteristics of the wall turbulence. In contrast, it can be observed that the turbulence intensity also takes the maximum a little far away from the bed in decelerated region.

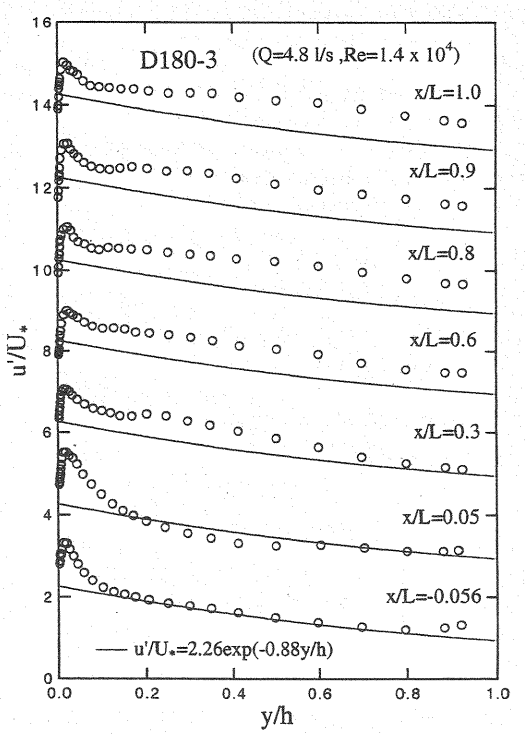

Figure 13 Distributions of Turbulence Intensity in Whole Depth

CONCLUSIONS

The turbulence measurements in open-channel flows with adverse pressure gradients were conducted accurately with a laser Doppler anemometer. The main findings in this study are as follows:

(1) In the region of $x/h_0 > 25$, the pressure gradient parameter does not change toward the downstream. Therefore, the flow is in equilibrium.

(2) The profiles of the streamwise velocity component in the inner- and outer-layers in the equilibrium region are expressed well by the log-wake law. The integration constant, van Driest's damping factor and wake strength parameter are affected by the pressure gradient. In contrast, von Karman constant is a truly universal constant.

(3) The shape of the turbulence intensity distributions u'/U_* in the viscous sublayer is almost linear. The gradient of this linear law increases with an increase of the pressure gradient parameter.

(4) The turbulence intensity takes a maximum not only very near the bed but also near half depth.

References

Clauser, F. H.: Turbulent boundary layers in adverse pressure gradients, *J. Aeronautical Sciences*, pp.91-108, 1954.

Coles, D.E.: The law of the wake in the turbulent boundary layer, *J. Fluid Mech.*, vol.1, pp.191-226, 1956.

Coles, D.E. and Hirst, E.A: *Proc. Computation of Turbulent Boundary Layers-1968, AFOSR-IFP-Stanford Conference*, Vol.II, Department of Mechanical Engineering, Stanford University, 1968.

Marusic, I., Uddin, A.K.M. and Perry, A.E.: Similarity law for the streamwise turbulence intensity in zero-pressure-gradient turbulent boundary layers, *Physics of Fluids*, Vol.9, No.12, pp.3718-3726, 1997.

Mellor, G.L. and Gibson, D.M.: Equilibrium turbulent boundary layers, *J. Fluid Mech.*, Vol.24, pp.225-253.1966

Nagano, Y., Tagawa, M. and Tsuji, T.: Effects of adverse pressure gradients on mean flows and turbulence statistics in a boundary layer, *Turbulent Shear Flows 8* (ed. F. Durst et al.), Springer-Verlag, Berlin Heidelberg, pp.7-21, 1993.

Nakagawa, H. and Nezu, I.: Bursting phenomenon near the wall in open-channel flows and its simple mathematical model, Memoirs, *Faculty of Eng., Kyoto University*, Vol40, pp.213-240, 1978.

Nezu, I. and Rodi, W.: Open-channel flow measurements with a laser Doppler anemometer, *J. Hydraulic Engineering*, ASCE, Vol.112, pp.335-355, 1986.

Nezu, I. and Nakagawa, H.: *Turbulence in Open-Channel Flows*, IAHR-Monograph, Balkema, 1993.

Nezu, I., Kadota, A. and Nakagawa, H.: Turbulent structure in accelerating and decelerating open-channel flows with laser Doppler anemometer, *9th Congress of the APD-IAHR*, Singapore, vol.1, pp.413-420, 1994.

Nezu, I., Kadota, A., He, J.X. and Toda, T.: Turbulent structures in open-channel flows over wavy boundary, *Flow Modeling and Turbulence Measurements* (eds. C.J. Chen et al.), Balkema, pp.91-98, 1996.

Okabe, T and Sugio, S.: Characteristics of two-dimensional flow with large depth-gradient, *Proceedings of Hydraulic Engineering*, Vol.25, JSCE, pp.119-124, 1981 (in Japanese).

Onitsuka, K., Ura, M., Akiyama, J. Okamoto, T. and Matsuoka, S.: Characteristics of open channel flows with adverse pressure gradients, *J. Hydraulic, Coastal and Environmental Engineering*, JSCE, No.558/II-38, pp.71-79, 1997, (in Japanese).

Onitsuka, K. and Nezu, I.: Turbulent structure in the near-wall region of 2-D open channel flows, *7th International Symposium on Flow Modeling and Turbulence Measurements*, Tainan, Taiwan, pp. 679-704, 1998..

Onitsuka, K., Nezu, I. and Fujita, M.: Effect of favorable pressure gradients on turbulent structure in open-channel flows, *Hydraulic Modeling*, (eds. Vijay P. Singh, II Won Seo, Jung H. Sonu), Water Resources Publications, LLC, USA, pp.3-16, 1999.

Song, T. and Graf, W.H.: Non-uniform open-channel flow over a rough bed, *Journal of Hydroscience and Hydraulic Engineering*, JSCE, Vol.12, pp.1-25, 1994.

Spalart, P.R. and Leonard, A.: Direct numerical simulation of equilibrium turbulent boundary layers, Turbulent Shear Flows 5(ed. F. Durst et al.), Springer-Verlag, Berlin Heidelberg, pp.234-252, 1987.

White, F.M.: *Viscous Fluid Flow*, McGraw Hill, 1974.

(Received August 22, 2000 ; revised December 22, 2000)